1   **Observations of N_2O_5 and $ClNO_2$ at a polluted urban surface site in North China: high N_2O_5**

2   **uptake coefficients and low $ClNO_2$ product yields**

3   Xinfeng Wang[a], Hao Wang[a], Likun Xue[a, *], Tao Wang[a, b], Liwei Wang[a], Rongrong Gu[a], Weihao

4   Wang[b], Yee Jun Tham[b], Zhe Wang[b], Lingxiao Yang[a], Jianmin Chen[a], Wenxing Wang[a]

5   [a] Environment Research Institute, Shandong University, Ji'nan, Shandong, China

6   [b] Department of Civil and Environmental Engineering, the Hong Kong Polytechnic University, Hong

7   Kong, China

8

9   * Correspondence author. Environment Research Institute, Shandong University, Ji'nan, China.

10   *E-mail addresses:* xuelikun@sdu.edu.cn (L. Xue).

11

12   **ABSTRACT**

13   Dinitrogen pentoxide (N_2O_5) and its heterogeneous uptake product, nitryl chloride ($ClNO_2$), play

14   important roles in the nocturnal boundary layer chemistry. To understand the abundances and

15   chemistry of N_2O_5 and $ClNO_2$ in the polluted urban atmosphere in North China, field measurements

16   were conducted by deploying a chemical ionization mass spectrometer in urban Ji'nan in September,

17   2014. The observed surface N_2O_5 concentrations were relatively low, with an average nocturnal

18   value of 22 pptv, although the source of NO_3 was rather strong, i.e., the NO_2 and O_3 were at very

19   high levels. The N_2O_5 concentration peaked in the early evening, which was associated with thermal

20   power plant plumes and residual O_3. Nocturnal N_2O_5 was lost very rapidly, mainly through

21   heterogeneous reactions on aerosol surfaces. The estimated N_2O_5 uptake coefficient was in the range

22   of 0.042 – 0.092, among the highest values obtained from ground based field measurements. The fast

heterogeneous reaction of N_2O_5 on high loadings of aerosols generated relatively high levels of $ClNO_2$, with an average nocturnal concentration of 132 pptv. Despite the rich chloride content in aerosols, the $ClNO_2$ product yield was low, 0.014 and 0.082 in two nighttime cases, much lower than the calculated values from the experiment-derived parameterization. The suppressed chlorine activation in polluted urban atmospheres was possibly associated with the reduced hygroscopicity, solubility, and activity of chloride in complex ambient aerosols.

1. Introduction

Dinitrogen pentoxide (N_2O_5) and nitryl chloride ($ClNO_2$) have been identified as important reactive nitrogen species in the polluted troposphere (Brown et al., 2006; Osthoff et al., 2008). N_2O_5 is produced reversibly from the nitrate radical (NO_3), which forms via the reaction of NO_2 with O_3 and normally accumulates at nighttime. It is removed through various chemical processes, including heterogeneous uptake of N_2O_5, photolysis of NO_3, reactions of NO_3 with NO and volatile organic compounds (VOCs), and so on (Brown and Stutz, 2012). In the nocturnal boundary layer, the loss of N_2O_5 is to a large extent controlled by heterogeneous reactions on sub-micrometer aerosols, leading to fine nitrate formation (Chang et al., 2011). In particular, the heterogeneous reactions of N_2O_5 on chloride-containing aerosols can release $ClNO_2$, which serves as an important source of Cl atoms and consequently contributes to the atmospheric oxidation capacity the next day (Tham et al., 2014; Thornton et al., 2010; Xue et al., 2015; Wang et al., 2016). Due to the significant effects of N_2O_5 and $ClNO_2$ on both particulate matter pollution and photochemical smog, close attention has been paid to their abundance as well as their chemistry in the past decade.

The heterogeneous removal of N_2O_5 and activation of $ClNO_2$ are governed by two key parameters, the N_2O_5 uptake coefficient (γ) and $ClNO_2$ product yield (ϕ). The uptake coefficient of N_2O_5 on aerosol surfaces varies with the aerosol composition. Acidic sulfates, chlorides, mineral substances, and liquid water in aerosols accelerate N_2O_5 uptake, whereas nitrates and organic matter exhibit a suppression effect (Bertram and Thornton, 2009; Brown et al., 2006; Morgan et al., 2015; Seisel et al., 2005). The $ClNO_2$ yield from N_2O_5 heterogeneous reactions strongly depends on the content of liquid water and dissolved chloride within the particles. Laboratory studies have developed a parameterization formula that fits the $ClNO_2$ yield as a function of chloride concentration and water content (Behnke et al., 1997; Bertram and Thornton, 2009; Roberts et al., 2009) and it is widely used in modeling studies (Sarwar et al., 2012 and 2014). Nevertheless, owing to the complexity of the real atmospheric environment and the various types of aerosol, field measurements have shown large variability in γ and ϕ values with location, and significant discrepancies have been found in the two values for ambient measurements and laboratory studies (Bertram and Thornton, 2009; Bertram et al., 2009; Osthoff et al., 2008; Phillips t al., 2016; Riedel et al., 2012; Riemer et al., 2009).

The complex nocturnal chemistry of N_2O_5 and $ClNO_2$ in polluted urban environments is of particular importance because of the intensive anthropogenic emissions of NO_x and VOCs from traffic and industry, the high levels of secondary pollutants of sub-micrometer aerosol and O_3, and the complicated ground surface owing to various types of land use. In the past decade, a number of field studies on N_2O_5 and $ClNO_2$ have been conducted in or over urban areas, downwind areas and polluted coastal sites, mainly in North America and Europe, revealing the large influence of anthropogenic activities. Elevated nocturnal concentrations of N_2O_5 (or NO_3) typically build up with high levels of O_3 and NO_2 but low levels of NO and humidity, whereas the loss and hence lifetime

are dominated by heterogeneous uptake of N_2O_5 and/or homogeneous reactions of NO_3 with anthropogenic VOCs (Asaf et al., 2009 and 2010; Benton et al., 2010; Brown et al., 2016; Wagner et al., 2013; Zheng et al., 2008). Tower and aircraft based measurements have shown that the concentration and chemistry of N_2O_5 across the boundary layer is strongly altitude dependent, with larger concentrations and longer lifetime at higher altitudes than those at the surface (Benton et al., 2010; Brown et al., 2007, 2009, 2013; Stutz et al., 2004 and 2010). The low levels of N_2O_5 at the urban surface are generally attributed to the abundant NO from freshly emitted vehicle exhausts, especially in the cold season (Benton et al., 2010; Zheng et al., 2008). Urban plumes and power plant plumes are apt to produce high levels of N_2O_5 and the heterogeneous product $ClNO_2$ at higher altitude because of the high concentrations of precursors and sometimes the high $ClNO_2$ yield (Brown et al., 2007 and 2013; Riedel et al., 2012 and 2013; Zaveri et al., 2010). Recent field measurements near megacities in East Asia also revealed high or very high levels of N_2O_5 and $ClNO_2$, which were attributed to the transport of urban/industrial plumes with abundant O_3 and NO_x and led to enhanced production of O_3 and RO_x radicals the following day (Brown et al., 2016; Tham et al., 2014 and 2016; Wang et al., 2016). Despite the above findings, few studies have been conducted on N_2O_5 and $ClNO_2$ in polluted urban environments in North China, where the atmospheric characteristics and chemistry may be unique.

Ji'nan, the capital city of Shandong province, is located close to the center of North China. It has a population of 7.0 million and 1.4 million vehicles in 2014 (Shandong Provincial Bureau of Statistics, http://www.stats-sd.gov.cn/tjnj/nj2014/indexch.htm). Due to the intensive emissions from industrial and other anthropogenic sources, Ji'nan and the surrounding areas have experienced severe particulate matter pollution and photochemical pollution in the past decade (Wang et al., 2014; Wen

89 et al., 2015; Sun et al., 2016). To understand the abundances of N_2O_5 and $ClNO_2$, the uptake

90 coefficient, and the product yield in urban areas of North China, simultaneous measurements of N_2O_5

91 and $ClNO_2$ were taken in urban Ji'nan in late summer of 2014. The concentrations and characteristics

92 of N_2O_5 and $ClNO_2$ were presented, and then the loss of N_2O_5 and the production of $ClNO_2$ were

93 analyzed and discussed in detail, with the expectation of obtaining a comprehensive understanding of

94 the chemistry of N_2O_5 and $ClNO_2$ in the polluted urban boundary layer in this region.

2. Experiments and methods

2.1. Site description

97 The measurement site is situated in urban Ji'nan (36°40′ N, 117°03′ E) in North China. The field

98 measurements were taken at the Urban Atmospheric Environment Observation Station (UAEOS) on

99 the 7th floor (~22 m above ground level) of a teaching building in the central campus of Shandong

100 University (SDU) from August 31 to September 21, 2014. The UAEOS-SDU site is surrounded by

101 dense buildings for teaching, living, and business, among which a number of trees are distributed.

102 There are major and minor roads nearby with a large traffic flow, especially in rush hour, and the

103 vehicles emit large amounts of NO_x into the atmosphere (mostly as NO). Some large-scale industries

104 are located in suburban areas (see Fig. 1). To the north and northeast of the UAEOS-SDU site, there

105 are several thermal power plants (TTP), two steel plants (SP), and one oil refinery plant (ORP). To

106 the southwest are several cement plants (CP) and a TTP. The coal-combustion industries near the site

107 emit smoke plumes containing abundant SO_2 and NO_x (usually dominated by NO_2).

2.2. Instruments and supporting data

109 N_2O_5 and $ClNO_2$ were simultaneously measured by iodide-chemical ionization mass spectrometry

110 (CIMS) (THS Instruments Inc., USA), which combines ion–molecule chemistry and mass

spectrometry (Kercher et al., 2009). The CIMS used in this study was the same one and had a similar setup to that in our previous studies at Mt. TMS in Hong Kong and at rural Wangdu in the North China Plain (Tham et al., 2016; Wang et al., 2016). Briefly, the sample inlet was installed ~1.5 m above the roof of the UAEOS-SDU site. Air samples were drawn through a 4-m PFA-Teflon tube (1/4″ O. D.) at a total flow rate of ~11 SLPM, and only 1.7 SLPM of the air flow was drawn into the CIMS for subsequent ion–molecule reactions and detection. All of the tubing and fittings were replaced daily with clean ones to avoid particle deposition and tubing loss. The abundance of N_2O_5 and $ClNO_2$ was quantified by the signals of $I(N_2O_5)^-$ at 235 amu and $I(ClNO_2)^-$ at 208 amu with a time resolution of 8 s. The N_2O_5 sensitivity was determined using the on-line synthetic method with standard N_2O_5 produced from reactions of NO_2 with O_3 (Bertram et al., 2009). The $ClNO_2$ sensitivity was determined by passing a known concentration of N_2O_5 through the NaCl slurry (Roberts et al., 2009). The background signals of the CIMS were examined periodically by forcing the sample flow through a filter packed with activated carbon and were generally low. For the detailed information on the measurement protocols and quality assurance and quality control procedures, please refer to Wang et al. (2016) and Tham et al. (2016).

Concurrently, several other trace gases were measured. NO (nitric oxide) and NO_2 were measured with a chemiluminescence NO_x analyzer (Model 42i, Thermo Environmental Instruments (TEI), USA) coupled with a highly selective photolytic converter (BLC, Meteorologie Consult GmbH, Germany), with detection limit of 0.05 ppbv for an integration time of 5 min (Xu et al., 2013). Ozone was measured with a commercial UV photometric instrument (Model 49i, TEI, USA). SO_2 was detected by the pulsed fluorescence method (Model 43C, TEI, USA) and CO was measured by the IR radiation absorption method (Model 300E, Teledyne Advanced Pollution Instrumentation (API),

133 USA). All of these gas analyzers were equipped with an inlet filter to prevent particles. They were

134 calibrated every three days with zero air and mixed standard gas.

135 Hourly $PM_{2.5}$ concentration data were obtained from the local air quality monitoring network

136 (http://58.56.98.78:8801/airdeploy.web/AirQuality/MapMain.aspx). The $PM_{2.5}$ at the site of Seed Co.,

137 Ltd. Shandong Province (SCL-SDP) was used in this study. This location is 1.8 km from our

138 AEOS-SDU site and has a similar surrounding environment. The on-line hourly $PM_{2.5}$ concentrations

139 from the SCL-SDP site were consistent with the off-line 12-hr data at the AEOS-SDU site and thus

140 were believed to be applicable. Aerosol surface area density (*A*) was estimated from the hourly $PM_{2.5}$

141 concentration, based on the linear correlation between $PM_{2.5}$ (measured by SHARP 5350, Thermal

142 Scientific, USA) and *A* (measured by WPS 1000XP, MSP, USA) obtained the same season in 2013

143 ($R^2 = 0.75$). Note that the sizes of aerosols measured by WPS in 2013 represent particle diameters

144 under nearly dry conditions. To take into account the hygroscopic growth of aerosols in high

145 humidity, the aerosol surface area data used in this study were corrected with a growth factor. The

146 growth factor was calculated by a parameterized formula expressed as a function of relative humidity

147 (RH): $GF = a(b + \frac{1}{(1-RH)})^{1/3}$ (Lewis, 2008). The values of *a* and *b* were 0.582 and 8.46 for the

148 nighttime periods based on the field measurements over the North China Plain by Achtert et al.

149 (2009). The estimated aerosol surface area density with consideration of the hygroscopic growth was

150 very high during this field campaign, in the levels of $3028 - 9194$ μm^2 cm^{-3}, which are comparable to

151 the measured aerosol surface area values in September, 2013. The uncertainty of the aerosol surface

152 area data used in this study was estimated to be ~30%.

153 Inorganic water-soluble ions in $PM_{2.5}$ were also measured in this study. $PM_{2.5}$ samples were

154 collected on quartz filters using a medium-volume sampler (TH-150, Tianhong, China) every 12

155   hours (08:00 to 20:00 local time for daytime samples and 20:00 to 08:00 for nighttime samples).

156   $PM_{2.5}$ filter samples were then dissolved completely in deionized water followed by ionic analysis by

157   ion chromatography (ICs-90, Dionex, USA). An AS14A Column and an AMMS 300 Suppressor

158   were used to detect anions including Cl^-, NO_3^-, and SO_4^{2-}. A CS12A Column and a CSRS Ultra II

159   Suppressor were used to detect cations including Na^+, NH_4^+, K^+, Mg^{2+}, and Ca^{2+}.

160   The liquid water and dissolved ion contents in $PM_{2.5}$ samples were calculated via an online aerosol

161   inorganics model (AIM-IV) (Wexler and Clegg, 2002), with input data of ambient concentrations of

162   major ions including H^+, NH_4^+, Na^+, SO_4^{2-}, NO_3^-, Cl^-, relative humidity, and temperature (T). The

163   AIM model can be run on the website http://www.uea.ac.uk/~e770/aim.html.

164   Due to lack of measurements data, the concentrations of 38 VOCs, including ethane, ethene,

165   ethyne, propane, propene, i-butane, n-butane, 1-butene, i-butene, trans-2-butene, cis-2-butene,

166   i-pentane, n-pentane, 1,3-butadiene, 1-pentene, isoprene, trans-2-pentene, cis-2-pentene,

167   3-methyl-1-butene, 2-methyl-1-butene, 2-methyl-2-butene, n-hexane, n-heptane, n-octane, n-nonane,

168   2,3-dimethylbutane, 2-methylpentane, 3-methylpentane, 2,4-dimethylpentane, 2,2,4-trimethylpentane,

169   cyclopentane, cyclohexane, benzene, toluene, ethylbenzene, m-xylene, p-xylene, and o-xylene, were

170   estimated based on other pollutant/parameter together with the correlationships. Specifically, the

171   concentrations of anthropogenic VOCs (37 VOCs except isoprene) were estimated according to the

172   measured CO concentrations and the linear relationships between VOCs and CO concentrations from

173   our previous field measurements at an urban site. The isoprene concentration was estimated

174   according to the measured temperature and the linear relationships between isoprene and ambient

175   temperature. The sum of the estimated concentrations of 38 VOCs was in the range of 11.8 – 126.8

176   ppbv.

177   In addition, meteorological parameters including temperature, relative humidity, wind speed and

178   direction were measured by a meteorological station (Huayun, China). NO_2 photolysis frequency

179   (j_{NO2}) was measured using a filter radiometer (Meteorologie Consult GmbH, Germany).

180   *2.3. Chemical reactions and calculations*

181   In the nocturnal boundary layer, NO_3 is mainly produced from the reaction of NO_2 with O_3 (R1),

182   with the reaction rate constant k_1 as a function of the ambient temperature. It further reacts with NO_2

183   to reversibly form N_2O_5 (R2), with a temperature-dependent equilibrium constant of K_{eq}. The

184   gas-phase loss of NO_3 primarily includes the reaction with NO (R3) with a temperature- dependent

185   reaction rate constant of k_3, and the oxidations of various VOCs (R4) with the NO_3 loss frequency k_4

186   as the sum of the products of each VOC concentration and the corresponding reaction rate constant.

187   The direct loss of N_2O_5 mainly depends on the heterogeneous uptake of N_2O_5 on aerosol surfaces

188   (R5), with the N_2O_5 loss frequency approximately as a function of the mean molecular speed, the

189   uptake coefficient, and the aerosol surface area density. Particularly, the heterogeneous reactions of

190   N_2O_5 on chloride-containing aerosols release $ClNO_2$ (R6), with the production rate coefficient k_6 as

191   the product of the $ClNO_2$ yield and the heterogeneous N_2O_5 loss frequency.

192    $$NO_2 + O_3 \xrightarrow{k_1} NO_3 + O_2 \quad\quad\quad\quad (R1)$$

193    $$NO_3 + NO_2 + M \xleftrightarrow{K_{eq}} N_2O_5 + M \quad\quad\quad\quad (R2)$$

194    $$NO_3 + NO \xrightarrow{k_3} 2NO_2 \quad\quad\quad\quad (R3)$$

195    $$NO_3 + VOCs \xrightarrow{k_4} products \quad\quad\quad\quad (R4)$$

196    $$N_2O_5 \xrightarrow{aerosols, k_5} products \quad\quad\quad\quad (R5)$$

197    $$N_2O_5 + Cl^- \xrightarrow{aerosols, k_6} ClNO_2 + NO_3^- \quad\quad\quad\quad (R6)$$

198   Under conditions of warm weather, stable air mass, and far from fresh NO_x source, the fast source

199 and loss processes of NO_3 and N_2O_5 as well as the rapid equilibrium between them are ready to

200 establish a near instantaneous steady state. As a result, the NO_3 concentration can be estimated with

201 the measured N_2O_5 concentration divided by the product of the equilibrium constant K_{eq} and the NO_2

202 concentration (see Eq. 1). The loss frequencies of N_2O_5 via indirect homogeneous reactions of NO_3

203 with NO and VOCs and via direct heterogeneous hydrolysis of N_2O_5 on aerosol surface can be

204 calculated according to Eq. 2, Eq. 3, and Eq. 4, respectively.

205 $$[NO_3] = \frac{[N_2O_5]}{K_{eq}[NO_2]} \qquad \text{(Eq. 1)}$$

206 $$L_{NO} = \frac{k_1[NO]}{K_{eq}[NO_2]} \qquad \text{(Eq. 2)}$$

207 $$L_{VOCs} = \frac{1.5 \times \sum_i (k_{VOC\_a,i}\ [VOC\_a]_i) + 3.5 \times k_{isoprene}[isoprene]}{K_{eq}[NO_2]} \qquad \text{(Eq. 3)}$$

208 $$L_{aerosol} \approx \frac{1}{4}\bar{c}\gamma A \qquad \text{(Eq. 4)}$$

209 Here, *[NO$_3$]*, *[N$_2$O$_5$]*, *[NO$_2$]*, and *[NO]* are the concentrations of NO_3, N_2O_5, NO_2, and NO,

210 respectively. *The [VOC_a]$_i$* and $k_{VOC\_a,\ i}$ stand for the concentration of one of the 37 anthropogenic

211 VOCs and the corresponding reaction rate constant with NO_3, respectively. The *[isoprene]* and

212 *$k_{isoprene}$* represent the isoprene concentration and the reaction rate constant with NO_3, respectively.

213 The $\bar{c}$, γ, and *A* are the mean molecular speed of N_2O_5, the N_2O_5 uptake coefficient, and the aerosol

214 surface area density, respectively. The reaction rate constants used in this study were all adopted

215 from the IUPAC (International Union of Pure and Applied Chemistry) website (Atkinson et al., 2004

216 and 2006). Note that to minimize the underestimation of loss of NO_3 and thus N_2O_5 through VOCs

217 oxidation caused by the limited species of VOCs estimated in *Section 2.2*, the calculated NO_3 loss

218 frequency arose from anthropogenic VOCs was enlarged by timing a factor of 1.5 and that arose

219 from biogenic VOCs was enlarged by timing a factor of 3.5 (Yan et al., 2005).

220   With assumption of a balance between the direct and indirect losses of NO_3 and N_2O_5 and their

221 production in steady state, the reciprocal of the steady-state lifetime of NO_3 can be expressed as the

222 sum of the indirect NO_3 loss frequency through heterogeneous uptake of N_2O_5 and the direct NO_3

223 loss frequency k_g via gas-phase reactions with NO and VOCs (see Eq. 5) (Brown et al., 2006;

224 Phillips et al., 2016). Therefore, if the $(\tau_{NO3})^{-1}$ exhibits a linear correlation with the $(K_{eq}[NO_2])$

225 during a selected period, the N_2O_5 uptake coefficient γ can be estimated based on the linear slope

226 between $(\tau_{NO3})^{-1}$ and $\frac{1}{4}\bar{c}AK_{eq}[NO_2]$.

227 $$(\tau_{NO3})^{-1} = \frac{[NO_3]}{k_1[NO_2][O_3]} = \frac{[N_2O_5]}{(k_1[NO_2][O_3])(K_{eq}[NO_2])}$$

228 $$= k_5(K_{eq}[NO_2]) + k_g \approx \frac{1}{4}\bar{c}\gamma A(K_{eq}[NO_2]) + k_g \qquad \text{(Eq. 5)}$$

229 Within a stable air mass (e.g., there are only relatively small variations in the primary and

230 precursor species), the increase in $ClNO_2$ concentration mainly arises from the $ClNO_2$ formation via

231 heterogeneous N_2O_5 reactions on chloride-containing aerosols. In such condition, the $ClNO_2$

232 production yield ϕ can be calculated from the production rate of $ClNO_2$ and the heterogeneous loss

233 rate of N_2O_5 (see Eq. 6).

234 $$\phi = \frac{d[ClNO_2]/dt}{\frac{1}{4}\bar{c}\gamma A[N_2O_5]} \qquad \text{(Eq. 6)}$$

235 **3. Observational results**

236 *3.1. Concentration levels*

237 Time series of hourly concentrations of N_2O_5, $ClNO_2$, other related pollutants, and the photolysis

238 frequency of NO_2 during the field campaign are shown in Fig. 2. Overall, N_2O_5 and $ClNO_2$

239 concentrations exhibited large variations from night to night. The average N_2O_5 and $ClNO_2$ mixing

240 ratios were 17 $\pm$ 11 pptv and 94 $\pm$ 58 pptv (average $\pm$ standard deviation). The mean nighttime

241 N_2O_5 concentration, 22 $\pm$ 13 pptv, was significantly higher than that for daytime. The maximum

242 hourly concentration of N_2O_5, 278 pptv, was recorded in the evening of September 5, with

243 corresponding NO_2 of 74.6 ppbv and O_3 of 55 ppbv. Compared with other locations in Asia, North

244 America, and Europe, urban Ji'nan had higher levels of precursors of NO_2 and O_3, but lower

245 concentrations of N_2O_5 (as shown in Table 1).

246 Compared to N_2O_5, the concentration of $ClNO_2$ at ground level in urban Ji'nan was moderately

247 high and exhibited a different variation pattern. The mean nocturnal concentration of $ClNO_2$ was 132

248 $\pm$ 43 pptv, and the maximum hourly mixing ratio reached 776 pptv, which appeared on the night of

249 September 7. The concentration peaks of $ClNO_2$ appeared with a time lag of 1–3 hours and lasted for

250 a much longer period than N_2O_5, possibly owing to its relatively long lifetime. The $ClNO_2$-to-N_2O_5

251 ratios in urban Ji'nan varied from several to dozens pptv/pptv, much higher than those observed in

252 other locations, such as the rural continental region (0.2–3) (Phillips et al., 2012) and an urban

253 background site (0.02–2.4) (Bannan et al., 2015).

254 During the measurement period of 22 days, there were 10 nights on which the N_2O_5 exhibited

255 apparent concentration peaks. To obtain a comprehensive understanding of the chemistry of N_2O_5

256 (and also $ClNO_2$) in urban Ji'nan, six nighttime cases (September 5, 6, 9, 12, 13, and 20) with

257 concurrent high concentration peaks of N_2O_5 and $ClNO_2$ but without an injection of freshly emitted

258 NO plumes, are analyzed in detail in the following sections.

3.2. Diurnal variations

260 The average diurnal variations of N_2O_5, $ClNO_2$, other trace gases, and meteorological parameters

261 are illustrated in Fig. 3. N_2O_5 exhibited a sharp concentration peak at 20:00 with an average

262 maximum value of 50 pptv, whereas $ClNO_2$ concentration presented a broad peak throughout the

263 night with the average maximum value appearing at 22:00. Compared with other field studies

264 (Brown et al., 2004; Wood et al., 2005), the N_2O_5 peak time in urban Ji'nan was relatively earlier.

NO and NO_2 had two concentration peaks in the rush hours in the morning and in the early evening. SO_2 concentration exhibited one daytime peak in the morning and one nighttime peak in the early evening—almost at the same time as the N_2O_5 peak. Ozone concentration showed a maximum at 15:00 in the afternoon, with a significant trough corresponding to the big NO peak in the morning. A relatively high level of residual O_3 was still present in the early evening when the N_2O_5 peaks appeared. The average ambient temperature was moderately high, ranging from 20.3 °C to 25.6 °C. The humidity was moderate, with RH varying from 57.5% to 79.0%.

3.3. Evening N_2O_5 peaks

To understand the origins of the evening N_2O_5 concentration peaks, we examined the 5-minute data of N_2O_5, $ClNO_2$, NO_x, SO_2, O_3, aerosol surface area density, relative humidity, temperature, and wind speed and direction in the six nighttime cases (shown in Fig. 4). The maximum 5-minute concentration of N_2O_5 (430 pptv) appeared at 20:45 on September 5, with concurrent 60.9 ppbv NO_2 and 61 ppbv O_3. In the early evening of September 5, the wind mainly originated from the north and the SO_2 mixing ratio stayed very high, with an average value of 57.9 ppbv, indicating that the polluted air mass was a coal combustion plume from thermal power plants in the north of Ji'nan (see Fig. 1). Once the wind changed to the south at 21:00, both NO and NO_2 concentrations increased rapidly followed by a gradual decrease in SO_2, suggesting that the air mass changed from a thermal power plant plume to a vehicle exhaust-dominated or mixed urban plume. As a result, the O_3 mixing ratio exhibited a sharp reduction and the N_2O_5 concentration dropped to a very low level. Similarly, the nighttime cases on September 6, 9, and 13 also exhibited high N_2O_5 concentration peaks (above 100 pptv) in the thermal power plant plumes (SO_2 exceeding 10 ppbv) and a sharp drop after the air masses changed (characterized by changes in wind direction and concentrations of NO_x and O_3).

13

287 Unlike the former four cases, the SO_2 concentrations were relatively low (mostly below 10 ppbv) in

288 the evenings of September 12 and 20, indicating weak influence from coal combustion plumes. At

289 this time, the NO_2 concentrations were moderate, at ~20 ppbv, which generated relatively low levels

290 of N_2O_5 with a peak concentration of ~40 pptv. In summary, the elevated evening concentration

291 peaks of N_2O_5 observed in urban Ji'nan were associated with northerly thermal power plant plumes

292 in which high concentrations of NO_2 and O_3 were present.

293 **4. Discussion**

294 *4.1 Estimation of N_2O_5 uptake coefficient*

295 To understand the loss of N_2O_5 and the heterogeneous uptake coefficient on aerosol surfaces,

296 $(\tau_{NO3})^{-1}$ were calculated according to Eq. 5, and scatter plots and linear regressions were made

297 between $(\tau_{NO3})^{-1}$ and $\frac{1}{4}\bar{c}AK_{eq}[NO_2]$ for selected periods in the six nighttime cases (see Fig. 5;

298 19:00-21:00 at the night of September 5, 19:00-06:00 at the night of September 6, 18:00-23:00 at the

299 night of September 9, 18:00-23:00 at the night of September 12, 18:00-23:00 at the night of

300 September 13, and 18:00-03:30 at the night of September 20). These periods were chosen with

301 relatively high and variable levels of N_2O_5 and NO_2, but very low concentration of NO which

302 indicates little influence from the fresh emission source of NO_x. During each period, the ambient

303 temperature was relatively high, averagely in the range of 21.0 – 27.3 °C. The wind speed was

304 generally low ($<$1.0 m s^{-1}) and the wind was often from the same direction, suggesting relatively

305 stable air masses. The air mass was confirmed to be in steady state by running a box model of MCM

306 v3.3 with consideration of both homogeneous and heterogeneous processes associated with NO_3 and

307 N_2O_5. The observed relevant pollutant concentrations and meteorological parameters as well as the

308 calculated uptake coefficient (see below) were taken as the inputs. The outputted N_2O_5 concentration

14

309   changed within a small range and appeared to be stabilizing within two minutes.

310   Based on the linear slopes of the scatter plots shown in Fig. 5 (correlation coefficients all above

311   0.82), the estimated N_2O_5 uptake coefficient γ were listed in Table 2, ranging from 0.042 to 0.092. As

312   shown, the γ values tended to increase with the rising humidity. At the nights of September 5 and 9,

313   the average RH was below 50% and the γ values were 0.042 and 0.061. At the nights of September 6,

314   12, 13, and 20, the RH rose to 57.2% – 71.6% and the γ values increased to 0.068 – 0.092. Compared

315   with other ground based field studies in West United states, Southwest Germany, and South China

316   (Bertram et al., 2009; Brown et al., 2016; Phillips et al., 2016; Riedel et al. 2012; Wagner et al.,

317   2013), the observed N_2O_5 uptake coefficients in this study are among the highest.

318   The estimated uptake coefficients were further used to calculate the loss frequencies of N_2O_5 via

319   heterogeneous hydrolysis (according to Eq. 4) during the six nighttime cases which were then

320   compared with the loss frequencies of the indirect removal pathways (calculated based on Eq. 2 and

321   Eq. 3). The direct N_2O_5 loss frequency via heterogeneous uptake for the selected periods was in the

322   range of 0.012 –0.030 s^{-1}. The heterogeneous loss frequency of N_2O_5 on aerosol surfaces contributed

323   three fourths (76.6%, on average) of the total N_2O_5 loss, mainly due to the high aerosol loading in

324   this region. The fast heterogeneous loss rate of N_2O_5 on aerosol surfaces caused rapid production of

325   particulate nitrate and gas-phase $ClNO_2$ (e.g., an increase of 10.3 $\mu g\ m^{-3}$ in fine nitrate concentration

326   and a sharp peak of 972 pptv $ClNO_2$ on the night of September 6, see Fig. 2). In consideration of the

327   high heterogeneous uptake coefficient of N_2O_5 on mineral substances (Karagulian et al., 2006; Seisel

328   et al., 2005) and the large surface area of urban ground (Baergen et al., 2015), the urban ground

329   surface might also contributed to the heterogeneous loss of N_2O_5. It has been reported that the ocean

330   surface contributed a large fraction to the loss of N_2O_5 in the coastal marine boundary layer (Kim et

331 al., 2014) and that the snow surface played an import role in the rapid loss of N_2O_5 at high latitudes

332 (Apodaca et al., 2008). The indirect loss frequency of N_2O_5 caused by VOCs oxidation by NO_3

333 varied from 0.002–0.009 s^{-1}, with an average contribution of 16.3%. The loss frequency through

334 gas-phase reaction of NO_3 with NO was between 0.0006 and 0.004 s^{-1}, contributing 7.1% to the total

335 N_2O_5 loss. For each period, the sum of the calculated indirect N_2O_5 loss frequencies were generally

336 consistent with the k_g divided by $K_{eq}[NO_2]$, further indicating the applicability of the inverse

337 lifetime analysis in estimation of N_2O_5 uptake coefficient. Overall, the removal of N_2O_5 in urban

338 Ji'nan was dominated by the fast heterogeneous reactions which led to a relatively low abundance of

339 N_2O_5 at the ground level.

340 *4.2 Derivation of ClNO$_2$ product yield*

341 To obtain a comprehensive understanding of the relatively high levels of $ClNO_2$ at ground level in

342 urban Ji'nan, we selected two proper periods at the nights of September 6 and 20 to calculate the

343 production yield of $ClNO_2$. As shown in Fig. 6, during the two selected periods of 20:35 – 21:50 on

344 September 6 and 20:00 – 1:30 on September 20, the wind directions were almost the same, from the

345 southeast or south. The humidity was relatively stable, with average RH of 65.7% and 58.8%. The

346 N_2O_5 concentration and the aerosol surface area density also exhibited small changes, with average

347 values of 50 and 36 pptv, and 7545 and 4124 μm^2 cm^{-3}, respectively. During these two periods, the

348 $ClNO_2$ concentration exhibited nearly linear increases, generating production rates of 8.40 and 0.55

349 ppt min^{-1}. According to Eq. 3 and the estimated N_2O_5 uptake coefficient, the derived production yield

350 in the two cases was 0.082 and 0.014, substantially lower than those observed in other locations

351 including the southeast coastline of the United States (0.1~0.65) (Osthoff et al., 2008) and

352 continental Colorado (0.07~0.36) (Thornton et al., 2010).

353   In addition, we compared the observed $ClNO_2$ yield with the parameterized calculation with the

354   data of liquid water content and aqueous chloride content. The concentration of chloride in fine

355   particles in urban Ji'nan was rather high (2.8 and 4.4 μg m^{-3} in the two nighttime cases), which

356   resulted in a high chloride content in aerosol liquid water (2.1 and 3.7 mol L^{-1}). As shown in Table 3,

357   the $ClNO_2$ yield observed in urban Ji'nan increased with rising relative humidity and chloride

358   content. Surprisingly, the observed $ClNO_2$ yields were much lower than those calculated via the

359   parameterized formula by Roberts et al. (2009). The lower values of observed $ClNO_2$ yield indicate

360   that the yields used in the modeling studies might be significantly overestimated, which should be

361   considered. The difference in $ClNO_2$ yield between field measurements and laboratory studies was

362   thought to be related to the altered dissolution of chloride in real atmospheric aerosols. This suggests

363   possible suppressed the hygroscopicity, solubility, and reactivity of chloride in complex ambient

364   aerosols due to internal mixing with or coated by water insoluble substances (Laskin et al., 2012; Li

365   et al., 2016; Semeniuk et al., 2007; Thornton et al., 2005; Ryder et al., 2014). Further studies are

366   required to clarify the causes.

367   **5. Summary and conclusions**

368   Field measurements of N_2O_5 and $ClNO_2$ were conducted in a polluted atmosphere at an urban site

369   in Ji'nan in North China from August 31 to September 21, 2014. During the measurement period, the

370   precursors of N_2O_5 (i.e., NO_2 and O_3) were abundant; however, the N_2O_5 concentration at ground

371   level was relatively low with an average nocturnal value of 22 pptv. The N_2O_5 concentration peaked

372   mostly in the evening, which was associated with coal combustion plumes emitted from thermal

373   power plants to the north of the city. Fast heterogeneous uptake was the main cause of the low levels

374   of N_2O_5 observed in urban Ji'nan. The estimated heterogeneous uptake coefficient of N_2O_5 from our

field study was rather high, in the range of 0.042 – 0.092, increasing positively with the ambient humidity. Furthermore, the fast heterogeneous reactions of N_2O_5 on chloride aerosols yielded moderately high levels of $ClNO_2$ with average nocturnal concentration of 132 pptv. The $ClNO_2$ yield was relatively low, 0.014 and 0.082 in two nighttime cases, increasing remarkably with rising humidity and chloride content. Notably, the observed $ClNO_2$ yield was significantly lower than those calculated from the laboratory parameterization formula, suggesting possible suppressed hygroscopicity, solubility, and activity of chloride in complex ambient aerosols.

Acknowledgments

References

Achtert, P., Birmili, W., Nowak, A., Wehner, B., Wiedensohler, A., Takegawa, N., Kondo, Y., Miyazaki, Y., Hu, M., Zhu, T., 2009. Hygroscopic growth of tropospheric particle number size distributions over the North China Plain. J. Geophys. Res. 114.

Apodaca, R.L., Huff, D.M., Simpson, W.R., 2008. The role of ice in N_2O_5 heterogeneous hydrolysis at high latitudes. Atmos. Chem. Phys. 8, 7451-7463.

Asaf, D., Pedersen, D., Matveev, V., Peleg, M., Kern, C., Zingler, J., Platt, U., Luria, M., 2009. Long-Term Measurements of NO_3 Radical at a Semiarid Urban Site: 1. Extreme Concentration Events and Their Oxidation Capacity. Environ. Sci. Technol. 43, 9117-9123.

Asaf, D., Tas, E., Pedersen, D., Peleg, M., Luria, M., 2010. Long-Term Measurements of NO_3

Radical at a Semiarid Urban Site: 2. Seasonal Trends and Loss Mechanisms. Environ. Sci. Technol. 44, 5901–5907.

Atkinson, R., Baulch, D., Cox, R., Crowley, J., Hampson, R., Hynes, R., Jenkin, M., Rossi, M., Troe, J., 2004. Evaluated kinetic and photochemical data for atmospheric chemistry: Volume I-gas phase reactions of O_x, HO_x, NO_x and SO_x species. Atmos. Chem. Phys. 4, 1461-1738.

Atkinson, R., Baulch, D., Cox, R., Crowley, J., Hampson, R., Hynes, R., Jenkin, M., Rossi, M., Troe, J., 2006. Evaluated kinetic and photochemical data for atmospheric chemistry: Volume II-gas phase reactions of organic species. Atmos. Chem. Phys. 6, 3625-4055.

Baergen, A.M., Styler, S., van Pinxteren, D., Müller, K., Herrmann, H., Donaldson, D.J., 2015. Chemistry of urban grime: Inorganic ion composition of grime vs. particles in Leipzig, Germany. Environ. Sci. Technol. 49, 12688–12696.

Bannan, T.J., Booth, A.M., Bacak, A., Muller, J., Leather, K.E., Le Breton, M., Jones, B., Young, D., Coe, H., Allan, J., 2015. The first UK measurements of nitryl chloride using a chemical ionization mass spectrometer in central London in the summer of 2012, and an investigation of the role of Cl atom oxidation. J. Geophys. Res. 120, 5638-5657.

Behnke, W., George, C., Scheer, V., Zetzsch, C., 1997. Production and decay of $ClNO_2$ from the reaction of gaseous N_2O_5 with NaCl solution: Bulk and aerosol experiments. J. Geophys. Res. 102, 3795-3804.

Benton, A.K., Langridge, J.M., Ball, S.M., Bloss, W.J., Dall'Osto, M., Nemitz, E., Harrison, R.M., Jones, R.L., 2010. Night-time chemistry above London: measurements of NO_3 and N_2O_5 from the BT Tower. Atmos. Chem. Phys. 10, 9781-9795.

Bertram, T.H., Thornton, J.A., 2009. Toward a general parameterization of N_2O_5 reactivity on

419   aqueous particles: the competing effects of particle liquid water, nitrate and chloride. Atmos.

420   Chem. Phys. 9, 8351-8363.

421   Bertram, T., Thornton, J., Riedel, T., Middlebrook, A., Bahreini, R., Bates, T., Quinn, P., Coffman,

422   D., 2009. Direct observations of N_2O_5 reactivity on ambient aerosol particles. Geophys. Res. Lett.

423   36, L19803.

424   Brown, S., Dibb, J., Stark, H., Aldener, M., Vozella, M., Whitlow, S., Williams, E., Lerner, B.,

425   Jakoubek, R., Middlebrook, A., 2004. Nighttime removal of NO_x in the summer marine boundary

426   layer. Geophys. Res. Lett 31, L07108.

427   Brown, S., Ryerson, T., Wollny, A., Brock, C., Peltier, R., Sullivan, A., Weber, R., Dube, W.,

428   Trainer, M., Meagher, J., 2006. Variability in nocturnal nitrogen oxide processing and its role in

429   regional air quality. Science 311, 67.

430   Brown, S., Dubé, W., Osthoff, H., Stutz, J., Ryerson, T., Wollny, A., Brock, C., Warneke, C., de

431   Gouw, J., Atlas, E., 2007. Vertical profiles in NO_3 and N_2O_5 measured from an aircraft: Results

432   from the NOAA P-3 and surface platforms during the New England Air Quality Study 2004. J.

433   Geophys. Res. 112, D22304.

434   Brown, S.S., Dubé, W.P., Fuchs, H., Ryerson, T.B., Wollny, A.G., Brock, C.A., Bahreini, R.,

435   Middlebrook, A.M., Neuman, J.A., Atlas, E., Roberts, J.M., Osthoff, H.D., Trainer, M.,

436   Fehsenfeld, F.C., Ravishankara, A.R., 2009. Reactive uptake coefficients for N_2O_5 determined

437   from aircraft measurements during the Second Texas Air Quality Study: Comparison to current

438   model parameterizations. J. Geophys. Res. 114, D00F10.

439   Brown, S.S., Stutz, J., 2012. Nighttime radical observations and chemistry. Chem. Soc. Rev. 41,

440   6405-6447.

441   Brown, S.S., Thornton, J.A., Keene, W.C., Pszenny, A.A.P., Sive, B.C., Dubé, W.P., Wagner, N.L.,

442   Young, C.J., Riedel, T.P., Roberts, J.M., VandenBoer, T.C., Bahreini, R., Öztürk, F., Middlebrook,

443   A.M., Kim, S., Hübler, G., Wolfe, D.E., 2013. Nitrogen, Aerosol Composition, and Halogens on a

444   Tall Tower (NACHTT): Overview of a wintertime air chemistry field study in the front range

445   urban corridor of Colorado. J. Geophys. Res. 118, 8067-8085.

446   Brown, S.S., Dubé, W.P., Tham, Y.J., Zha, Q., Xue, L., Poon, S., Wang, Z., Blake, D.R., Tsui, W.,

447   Parrish, D.D., Wang, T., 2016. Nighttime chemistry at a high altitude site above Hong Kong. J.

448   Geophys. Res. 121, 2457–2475.

449   Chang, W.L., Bhave, P.V., Brown, S.S., Riemer, N., Stutz, J., Dabdub, D., 2011. Heterogeneous

450   Atmospheric Chemistry, Ambient Measurements, and Model Calculations of N_2O_5: A Review.

451   Aerosol Sci. Tech. 45, 665 - 695.

452   Crowley, J.N., Schuster, G., Pouvesle, N., Parchatka, U., Fischer, H., Bonn, B., Bingemer, H.,

453   Lelieveld, J., 2010. Nocturnal nitrogen oxides at a rural mountain-site in south-western Germany.

454   Atmos. Chem. Phys. 10, 2795-2812.

455   Crowley, J.N., Thieser, J., Tang, M.J., Schuster, G., Bozem, H., Beygi, Z.H., Fischer, H., Diesch,

456   J.M., Drewnick, F., Borrmann, S., Song, W., Yassaa, N., Williams, J., Pöhler, D., Platt, U.,

457   Lelieveld, J., 2011. Variable lifetimes and loss mechanisms for NO_3 and N_2O_5 during the

458   DOMINO campaign: contrasts between marine, urban and continental air. Atmos. Chem. Phys. 11,

459   10853-10870.

460   Huff, D.M., Joyce, P.L., Fochesatto, G.J., Simpson, W.R., 2011. Deposition of dinitrogen pentoxide,

461   N_2O_5, to the snowpack at high latitudes. Atmos. Chem. Phys. 11, 4929-4938.

462   Karagulian, F., Santschi, C., Rossi, M.J., 2006. The heterogeneous chemical kinetics of N_2O_5 on

463   CaCO$_3$ and other atmospheric mineral dust surrogates. Atmos. Chem. Phys. 6, 1373-1388.

464   Kercher, J., Riedel, T., Thornton, J., 2009. Chlorine activation by N$_2$O$_5$: simultaneous, in situ

465   detection of ClNO$_2$ and N$_2$O$_5$ by chemical ionization mass spectrometry. Atmos. Meas. Tech. 2,

466   193-204.

467   Kim, M.J., Farmer, D.K., Bertram, T.H., 2014. A controlling role for the air−sea interface in the

468   chemical processing of reactive nitrogen in the coastal marine boundary layer. Proc. Natl. Acad.

469   Sci. 111, 3943-3948.

470   Laskin, A., Moffet, R.C., Gilles, M.K., Fast, J.D., Zaveri, R.A., Wang, B., Nigge, P., Shutthanandan,

471   J., 2012. Tropospheric chemistry of internally mixed sea salt and organic particles: Surprising

472   reactivity of NaCl with weak organic acids. J. Geophys. Res. 117, D15302.

473   Lewis, E.R., 2008. An examination of Köhler theory resulting in an accurate expression for the

474   equilibrium radius ratio of a hygroscopic aerosol particle valid up to and including relative

475   humidity 100%. J. Geophys. Res. 113.

476   Li, W., Shao, L., Zhang, D., Ro, C.-U., Hu, M., Bi, X., Geng, H., Matsuki, A., Niu, H., Chen, J.,

477   2016. A review of single aerosol particle studies in the atmosphere of East Asia: morphology,

478   mixing state, source, and heterogeneous reactions. J. Clean Prod. 112, Part 2, 1330-1349.

479   Matsumoto, J., Imai, H., Kosugi, N., Kajii, Y., 2005. In situ measurement of N$_2$O$_5$ in the urban

480   atmosphere by thermal decomposition/laser-induced fluorescence technique. Atmos. Environ. 39,

481   6802-6811.

482   Morgan, W.T., Ouyang, B., Allan, J.D., Aruffo, E., Di Carlo, P., Kennedy, O.J., Lowe, D., Flynn,

483   M.J., Rosenberg, P.D., Williams, P.I., Jones, R., McFiggans, G.B., Coe, H., 2015. Influence of

484   aerosol chemical composition on N$_2$O$_5$ uptake: airborne regional measurements in northwestern

485   Europe. Atmos. Chem. Phys. 15, 973-990.

486   Osthoff, H.D., Roberts, J.M., Ravishankara, A.R., Williams, E.J., Lerner, B.M., Sommariva, R.,

487   Bates, T.S., Coffman, D., Quinn, P.K., Dibb, J.E., Stark, H., Burkholder, J.B., Talukdar, R.K.,

488   Meagher, J., Fehsenfeld, F.C., Brown, S.S., 2008. High levels of nitryl chloride in the polluted

489   subtropical marine boundary layer. Nature Geosci. 1, 324-328.

490   Phillips, G.J., Tang, M.J., Thieser, J., Brickwedde, B., Schuster, G., Bohn, B., Lelieveld, J., Crowley,

491   J.N., 2012. Significant concentrations of nitryl chloride observed in rural continental Europe

492   associated with the influence of sea salt chloride and anthropogenic emissions. Geophys. Res. Lett.

493   39, L10811.

494   Phillips, G.J., Thieser, J., Tang, M., Sobanski, N., Schuster, G., Fachinger, J., Drewnick, F.,

495   Borrmann, S., Bingemer, H., Lelieveld, J., Crowley, J.N., 2016. Estimating N_2O_5 uptake

496   coefficients using ambient measurements of NO_3, N_2O_5, $ClNO_2$ and particle-phase nitrate. Atmos.

497   Chem. Phys 16, 13231-13249.

498   Riedel, T.P., Bertram, T.H., Ryder, O.S., Liu, S., Day, D.A., Russell, L.M., Gaston, C.J., Prather,

499   K.A., Thornton, J.A., 2012. Direct N_2O_5 reactivity measurements at a polluted coastal site. Atmos.

500   Chem. Phys. 12, 2959-2968.

501   Riedel, T.P., Wagner, N.L., Dubé, W.P., Middlebrook, A.M., Young, C.J., Öztürk, F., Bahreini, R.,

502   VandenBoer, T.C., Wolfe, D.E., Williams, E.J., Roberts, J.M., Brown, S.S., Thornton, J.A., 2013.

503   Chlorine activation within urban or power plant plumes: Vertically resolved $ClNO_2$ and Cl_2

504   measurements from a tall tower in a polluted continental setting. J. Geophys. Res. 118, 8702-8715.

505   Riemer, N., Vogel, H., Vogel, B., Anttila, T., Kiendler-Scharr, A., Mentel, T., 2009. Relative

506   importance of organic coatings for the heterogeneous hydrolysis of N_2O_5 during summer in

507   Europe. J. Geophys. Res. 114, D17307.

508   Roberts, J.M., Osthoff, H.D., Brown, S.S., Ravishankara, A., Coffman, D., Quinn, P., Bates, T., 2009.

509   Laboratory studies of products of N_2O_5 uptake on Cl containing substrates. Geophys. Res. Lett. 36,

510   L20808.

511   Ryder, O.S., Ault, A.P., Cahill, J.F., Guasco, T.L., Riedel, T.P., Cuadra-Rodriguez, L.A., Gaston,

512   C.J., Fitzgerald, E., Lee, C., Prather, K.A., Bertram, T.H., 2014. On the Role of Particle Inorganic

513   Mixing State in the Reactive Uptake of N_2O_5 to Ambient Aerosol Particles. Environ. Sci. Technol.

514   48, 1618-1627.

515   Sarwar, G., Simon, H., Bhave, P., Yarwood, G., 2012. Examining the impact of heterogeneous nitryl

516   chloride production on air quality across the United States. Atmos. Chem. Phys. 12, 6455-6473.

517   Sarwar, G., Simon, H., Xing, J., Mathur, R., 2014. Importance of tropospheric $ClNO_2$ chemistry

518   across the Northern Hemisphere. Geophys. Res. Lett. 41, 4050-4058.

519   Seisel, S., Börensen, C., Vogt, R., Zellner, R., 2005. Kinetics and mechanism of the uptake of N_2O_5

520   on mineral dust at 298 K. Atmos. Chem. Phys. 5, 3423-3432.

521   Semeniuk, T.A., Wise, M.E., Martin, S.T., Russell, L.M. and Buseck, P.R., 2007. Hygroscopic

522   Behavior of Aerosol Particles from Biomass Fires Using Environmental Transmission Electron

523   Microscopy. J. Atmos. Chem. 56, 259-273.

524   Stutz, J., Alicke, B., Ackermann, R., Geyer, A., White, A., Williams, E., 2004. Vertical profiles of

525   NO_3, N_2O_5, O_3, and NO_x in the nocturnal boundary layer: 1. Observations during the Texas Air

526   Quality Study 2000. J. Geophys. Res. 109, D12306.

527   Stutz, J., Wong, K.W., Lawrence, L., Ziemba, L., Flynn, J.H., Rappenglück, B., Lefer, B., 2010.

528   Nocturnal NO_3 radical chemistry in Houston, TX. Atmos. Environ. 44, 4099-4106.

529   Sun, L., Xue, L.K., Wang,T., Gao, J., Ding, A.J., Cooper, O.W., Lin, M.Y., Xu, P.J., Wang, Z.,

530   Wang, X.F., Wen, L., Zhu, Y.H., Chen. T.S., Yang, L.X., Wang, Y., Chen. J.M., and Wang, W.X.,

531   2016. Significant increase of summertime ozone at Mount. Tai in Central Eastern China, Atmos.

532   Chem. Phys. 16, 10637-10650.

533   Tham, Y., Yan, C., Xue, L., Zha, Q., Wang, X., Wang, T., 2014. Presence of high nitryl chloride in

534   Asian coastal environment and its impact on atmospheric photochemistry. Chinese. Sci. Bull. 59,

535   356-359.

536   Tham, Y.J., Wang, Z., Li, Q., Yun, H., Wang, W., Wang, X., Xue, L., Lu, K., Ma, N., Bohn, B., Li,

537   X., Kecorius, S., Größ, J., Shao, M., Wiedensohler, A., Zhang, Y., Wang, T., 2016. Significant

538   concentrations of nitryl chloride sustained in the morning: Investigations of the causes and impacts

539   on ozone production in a polluted region of northern China. Atmos. Chem. Phys. Discuss. 2016,

540   1-34.

541   Thornton, J., Abbatt, J., 2005. N_2O_5 reaction on submicron sea salt aerosol: Kinetics, products, and

542   the effect of surface active organics. J. Phys. Chem. A 109, 10004-10012.

543   Thornton, J., Kercher, J., Riedel, T., Wagner, N., Cozic, J., Holloway, J., DubÃ, W., Wolfe, G.,

544   Quinn, P., Middlebrook, A., 2010. A large atomic chlorine source inferred from mid-continental

545   reactive nitrogen chemistry. Nature 464, 271-274.

546   Wagner, N.L., Riedel, T.P., Young, C.J., Bahreini, R., Brock, C.A., Dubé, W.P., Kim, S.,

547   Middlebrook, A.M., Öztürk, F., Roberts, J.M., Russo, R., Sive, B., Swarthout, R., Thornton, J.A.,

548   VandenBoer, T.C., Zhou, Y., Brown, S.S., 2013. N_2O_5 uptake coefficients and nocturnal NO_2

549   removal rates determined from ambient wintertime measurements. J. Geophys. Res. 118,

550   9331-9350.

551   Wang, S., Shi, C., Zhou, B., Zhao, H., Wang, Z., Yang, S., Chen, L., 2013. Observation of NO_3

552   radicals over Shanghai, China. Atmos. Environ. 70, 401-409.

553   Wang, T., Tham, Y.J., Xue, L., Li, Q., Zha, Q., Wang, Z., Poon, S.C.N., Dubé, W.P., Blake, D.R.,

554   Louie, P.K.K., Luk, C.W.Y., Tsui, W., Brown, S.S., 2016. Observations of nitryl chloride and

555   modeling its source and effect on ozone in the planetary boundary layer of southern China. J.

556   Geophys. Res. 121, 2476-2489.

557   Wang, X., Chen, J., Sun, J., Li, W., Yang, L., Wen, L., Wang, W., Wang, X., Collett Jr, J.L., Shi, Y.,

558   Zhang, Q., Hu, J., Yao, L., Zhu, Y., Sui, X., Sun, X., Mellouki, A., 2014. Severe haze episodes

559   and seriously polluted fog water in Ji'nan, China. Sci. Total. Environ. 493, 133-137.

560   Wen, L., Chen, J., Yang, L., Wang, X., Caihong, X., Sui, X., Yao, L., Zhu, Y., Zhang, J., Zhu, T.,

561   Wang, W., 2015. Enhanced formation of fine particulate nitrate at a rural site on the North China

562   Plain in summer: the important roles of ammonia and ozone. Atmos. Environ. 101, 294-302.

563   Wexler, A.S., Clegg, S.L., 2002. Atmospheric aerosol models for systems including the ions H^+,

564   NH_4^+, Na^+, SO_4^{2-}, NO_3^-, Cl^-, Br^-, and H_2O. J. Geophys. Res. 107, 4207.

565   Wood, E.C., Bertram, T.H., Wooldridge, P.J., Cohen, R.C., 2005. Measurements of N_2O_5, NO_2, and

566   O_3 east of the San Francisco Bay. Atmos. Chem. Phys. 5, 483-491.

567   Xu, Z., Wang, T., Xue, L.K., Louie, P.K.K., Luk, C.W.Y., Gao, J., Wang, S.L., Chai, F.H., Wang,

568   W.X., 2013. Evaluating the uncertainties of thermal catalytic conversion in measuring atmospheric

569   nitrogen dioxide at four differently polluted sites in China. Atmos. Environ. 76, 221-226.

570   Xue, L.K., Saunders, S.M., Wang, T., Gao, R., Wang, X.F., Zhang, Q.Z., Wang, W.X., 2015.

571   Development of a chlorine chemistry module for the Master Chemical Mechanism. Geosci. Model

572   Dev. 8, 3151-3162.

573 Yan, Y., Wang, Z., Bai, Y., Xie, S., Shao, M., 2005. Establishment of vegetation VOC emission

574   inventory in China. China Environmental Science 25, 110-114 (in Chinese).

575 Zaveri, R.A., Berkowitz, C.M., Brechtel, F.J., Gilles, M.K., Hubbe, J.M., Jayne, J.T., Kleinman, L.I.,

576   Laskin, A., Madronich, S., Onasch, T.B., Pekour, M.S., Springston, S.R., Thornton, J.A., Tivanski,

577   A.V., Worsnop, D.R., 2010. Nighttime chemical evolution of aerosol and trace gases in a power

578   plant plume: Implications for secondary organic nitrate and organosulfate aerosol formation, NO_3

579   radical chemistry, and N_2O_5 heterogeneous hydrolysis. J. Geophys. Res. 115, D12304.

580 Zheng, J., Zhang, R., Fortner, E.C., Volkamer, R.M., Molina, L., Aiken, A.C., Jimenez, J.L.,

581   Gaeggeler, K., Dommen, J., Dusanter, S., Stevens, P.S., Tie, X., 2008. Measurements of HNO_3

582   and N_2O_5 using   ion   drift-chemical   ionization   mass   spectrometry   during   the

583   MILAGRO/MCMA-2006 campaign. Atmos. Chem. Phys. 8, 6823-6838.

584 **Table 1.** Peak concentrations of N_2O_5 and the corresponding NO_2 and O_3 concentrations observed in

585 Ji'nan and other locations.

Location	Type	Instrument	Height	N_2O_5 (pptv)	NO_2 (ppbv)	O_3 (ppbv)	Reference
East coast of USA	Coastal	CaRDS	Sea level	175	6	35	*Brown et al.*, 2004
California, USA	coastal	LIF	290m asl.	200	13	14	*Wood et al.*, 2005
Tokyo, Japan	urban	LIF	130m asl	800	70	3	*Matsumoto et al.*, 2005
Mexico City, Mexico	urban	ID-CIMS	30m agl	60	42	22	*Zheng et al.*, 2008
London, England	urban	LED-BBCEAS	160m agl	450	14	14	*Benton et al.*, 2010
Taunus, Germany	mountain	OA-CRDS	825m asl	550	2	50	*Crowley et al.*, 2010
Southern Spain	coastal	CaRDS	5-10m agl	400	10	25	*Crowley et al.*, 2011
Fairbanks, USA	High latitude	CRDS	400 asl	80	10	20	*Huff et al.*, 2011
Shanghai, China	urban	DOAS	20m agl	3250	22.5	50	*Wang et al.*, 2013
Mt. TMS, HK	mountain	CIMS	975 m asl	8000	11	60	*Wang et al.*, 2016
Northwestern Europe	airborne	BBCEAS	--	670	6.2	42	*Morgan et al.*, 2015
Ji'nan, China	urban	CIMS	22m agl	278	74.6	55	This study

586

28

587 **Table 2.** Estimated uptake coefficient of N_2O_5 and related parameters for selected periods in six

588 nighttime cases.

Nighttime case	T (^{o} C)	RH (%)	N_2O_5 (pptv)	γ	k_g (s^{-1})	Correlation coefficient
Sep. 5	27.3	43.4	213	0.042	0.2784	0.82
Sep. 6	24.9	66.0	57	0.068	0.0792	0.88
Sep. 9	25.4	46.2	83	0.061	0.0801	0.88
Sep. 12	21.0	71.6	29	0.069	0.3763	0.85
Sep. 13	24.6	58.5	48	0.092	0.0049	0.85
Sep. 20	23.9	57.9	33	0.081	0.0241	0.91

589

590 **Table 3.** Observation and parameterization based $ClNO_2$ yield and related parameters for selected

591 periods in two nighttime cases.

Nighttime case	RH (%)	$ClNO_2$ (pptv)	Cl^-(air) $\mu g\ m^{-3}$	Cl^-(aq) (mol L^{-1})	Observed ϕ	Parameterized $\phi*$
Sep. 6	65.7	508	4.4	2.1	0.082	0.945
Sep. 20	58.8	115	2.8	3.7	0.014	0.968

592

Figure captions

Figure 1. Location of Ji'nan & the sampling site, where some large industries are operated.

Figure 2. Time series of hourly concentrations of N_2O_5, $ClNO_2$, other related pollutants, and NO_2 photolysis frequency.

Figure 3. Diurnal variations of N_2O_5, $ClNO_2$, other related pollutants and parameters for the whole campaign. Error bar represents standard error.

Figure 4. Time series of gases, aerosol surface area density, and meteorological parameters for six evening N_2O_5 peaks on September 5, 6, 9, 12, 13 and 20.

Figure 5. N_2O_5 uptake coefficients derived from scatter plots of $\tau(NO_3)^{-1}$ versus $0.25cAK_{eq}\times[NO_2]$ for six selected periods on the nights of September 5, 6, 9, 12, 13 and 20.

Figure 6. Time series of wind, relative humidity, N_2O_5 and $ClNO_2$ concentrations, and aerosol surface area density, for two nighttime cases on September 6 and 20, showing nearly linear increase of $ClNO_2$.
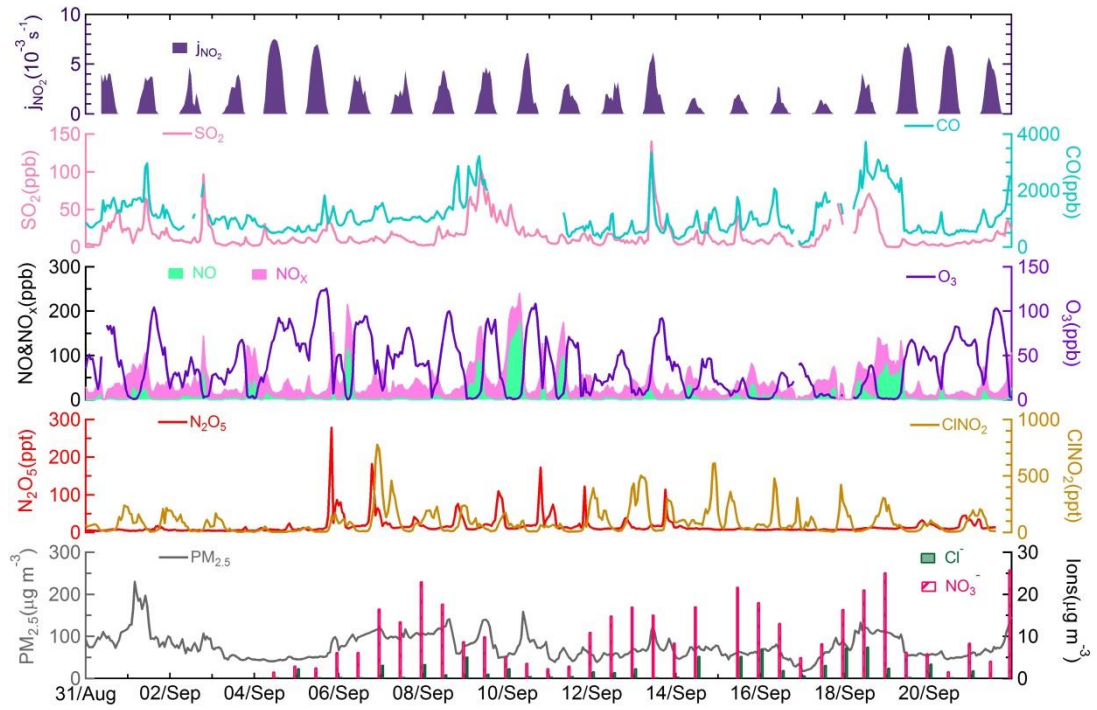
607
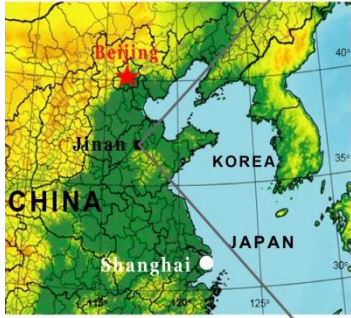
TPP:thermal power plant, SP:steel plant, ORP:oil refinery plant, CP:cement plant
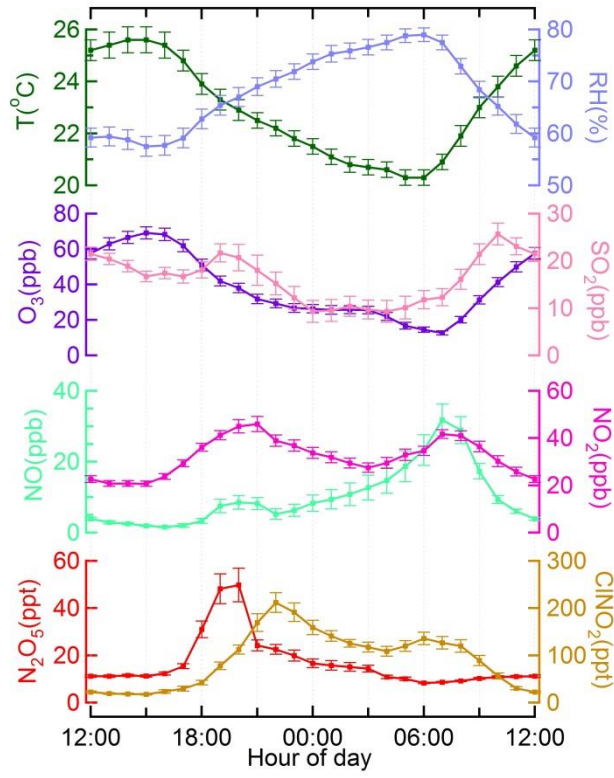
608   **Figure 1.**
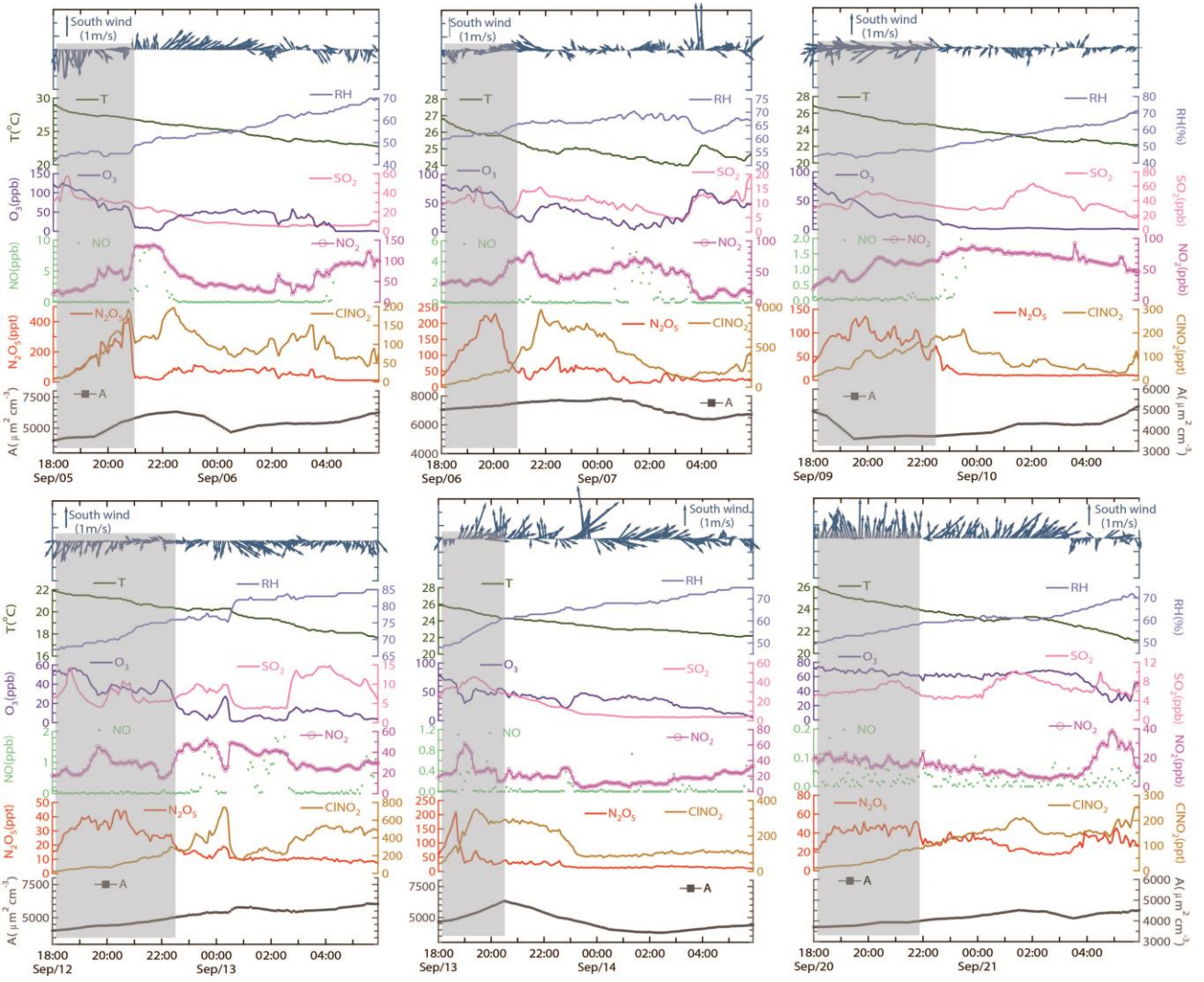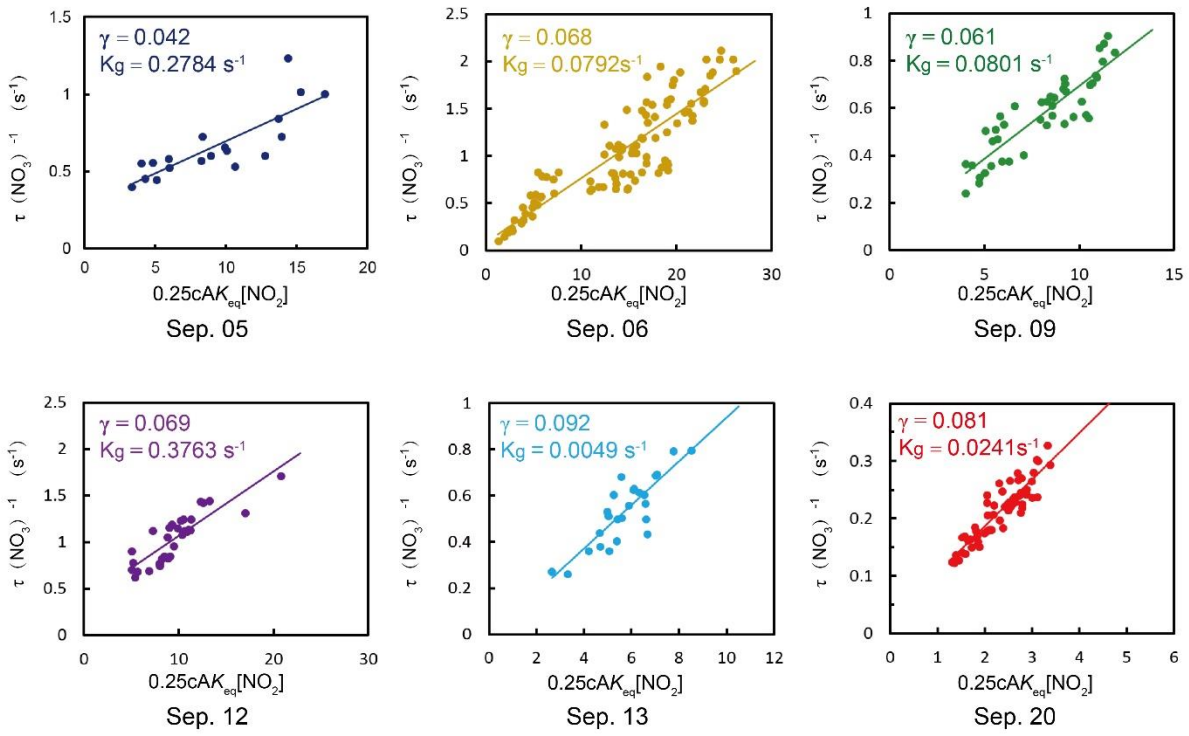
609

Figure 2.

611

Figure 3.

Figure 4.

Figure 5.

618

619

620   **Figure 6.**